Low-temperature behaviour of the six-state clock model with competing interactions

1993 J. Phys. A: Math. Gen. 26 4887

(http://iopscience.iop.org/0305-4470/26/19/021)

J. Phys. A: Math. Gen. **26** (1993) 4887–4905. Printed in the UK

Low-temperature behaviour of the six-state clock model with competing interactions

F Seno, D A Rabson† and J M Yeomans

Theoretical Physics, University of Oxford, 1 Keble Road, Oxford OX1 3NP, UK

Received 23 February 1993

Abstract. The phase diagram of the six-state clock model on a three-dimensional lattice, with first- and second-neighbour competing interactions along one direction, is analysed using a systematic low-temperature expansion carried to all orders where necessary. A transfer-matrix method simplifies the configurational analysis. We find that an infinite number of commensurate phases are stable near a zero-temperature multiphase point; a richer hierarchy of 'mixed' phases is found to be stable down to zero temperature than in the ANNNI model. The system corresponds to an *XY* model with infinite hexagonal anisotropy and may be relevant to rare-earth multilayers.

1. Introduction

Rare-earth metals show an interesting variety of magnetic phases, many with long wavelengths that can be commensurate or incommensurate with the underlying lattice. Recent work in rare-earth multilayers has rekindled interest in these systems (see e.g. Majkrzak *et al* 1991 and references therein). The bulk phase diagrams of the rare-earth metals holmium, dysprosium, and terbium display regions with helical (i.e. easy-plane) spin order; these have been described with an XY model including competing, temperature-dependent ferromagnetic and antiferromagnetic interactions along the axis of the helix and six-fold anisotropy (Yoshimori 1959)†. Previous work has used mean-field theory and concentrated on fixing the exchange parameters at values appropriate to the experimental systems (Jensen and Mackintosh 1991). A different approach now seems useful: by elucidating the phase diagram of these models for more general values of the couplings, we hope to predict ways in which multilayers displaying new physics can be fabricated.

This paper takes a first step along this path by considering the low-temperature behaviour of the six-state clock model on a three-dimensional lattice with first- and second-neighbour competing interactions along the axial direction. This system corresponds to an XY model with infinite hexagonal anisotropy. We find that an infinite number of commensurate phases are stable near a zero-temperature multiphase point.

† Current address: MS B262, Los Alamos National Laboratory, Los Alamos, NM 87545, USA.

‡ In bulk, the helical phase is replaced at low temperatures with conical ordering, in which the spins acquire a component perpendicular to the easy plane. Within our model, this extra component plays no role (except in altering the temperature dependence of the parameters J, defined below). It is worth noting that even very thick (5000 Å) films of Ho grown by molecular epitaxy appear to stay in the helical phase down to zero temperature (Jehan *et al* 1993).

0305-4470/93/194887+19 $07.50

2. The model and its ground states

The three-dimensional, six-state clock model with competing axial interactions J_1 and J_2 is described by the Hamiltonian

$$H=-\frac{1}{2}J_0\sum_{j,\alpha,\beta(\alpha)}\cos\left(\frac{2\pi}{6}(n_{j\alpha}-n_{j\beta})\right)-J_1\sum_{j,\alpha}\cos\left(\frac{2\pi}{6}(n_{j\alpha}-n_{j+1,\alpha})\right)$$
$$+J_2\sum_{j,\alpha}\cos\left(\frac{2\pi}{6}(n_{j\alpha}-n_{j+2,\alpha})\right) \tag{1}$$

where the Roman index j labels the planes of spins perpendicular to the axial direction and the Greek indices the spins within each plane. The first term sums over each spin α in plane j and each in-plane nearest neighbour β of α. The integers $n_{j\alpha}$ assume the values 0, 1, 2, 3, 4, and 5, representing spins lying in the planes and pointing at angles $2\pi n_{j\alpha}/6$ relative to the x axis. Each spin has unit magnitude. By taking the in-plane coupling to be ferromagnetic (J_0 positive), we ensure that at zero temperature all spins within any given plane point in the same direction. We can also take J_1 to be positive (ferromagnetic), because the problem with an antiferromagnetic first-neighbour axial interaction maps on to the ferromagnetic problem but with the spins in every second layer rotated by π. We consider only positive (antiferromagnetic) values for the second-axial-neighbour interaction J_2, as the completely unfrustrated ferromagnetic system displays no interesting behaviour.

The aim is to construct the low-temperature phase diagram of this model as a function of $x=J_2/J_1$ and of the temperature, T. For a given rare earth, the effective interactions J_0, J_1, and J_2 depend on temperature, pressure, and, in multilayers and thin films, the layer thickness (Jensen and Mackintosh 1991). Varying one of these parameters then describes a one-dimensional trajectory in the two-dimensional phase space of J_2/J_1 against T (see figure 1).

One easily verifies the ground states of the Hamiltonian (1) as a function of x. Since the in-plane coupling is ferromagnetic, we can represent each plane of spins as a single number n_j along the axial chain; thus we represent the ferromagnetic phase that prevails at $T=0$ for $x<\frac{1}{3}$ by

$$\ldots 00000\ldots \tag{2}$$

understanding the inclusion of the other, equivalent, ferromagnetic phases, $\ldots 22222\ldots$ and so forth. For $\frac{1}{3}<x<1$, the ground state has axial ordering

$$\ldots 012345012345\ldots \tag{3}$$

again including equivalent orderings such as $\ldots 321054\ldots$. For $x>1$, the ground states

$$\ldots 013401340134\ldots \tag{4}$$

and

$$\ldots 003300330033\ldots \tag{5}$$

are degenerate. We shall see, however, that any non-zero temperature will lift this degeneracy in favour of (5).

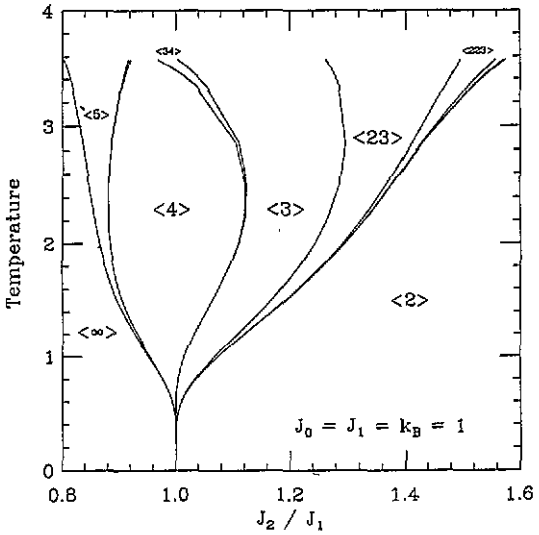

Figure 1. Results from mean-field theory. Along the horizontal axis is plotted the ratio of the antiferromagnetic next-nearest-neighbour and ferromagnetic nearest-neighbour axial bond strengths. For the purposes of this figure, we have set $J_0 = J_1$ and $z = 6$. The vertical axis is temperature in units of $J_0/k_B T$. The Curie–Weiss temperature above which there is no net magnetization in the planes is 3.9 at the left side of the graph, 4.6 at the right side. We numerically and iteratively consider pairs of stable phases at their coexistence line, as determined in the previous iteration, and their 'child' phase (e.g. ⟨23⟩ from parents ⟨2⟩ and ⟨3⟩). Numerically, it appears that phases not formed in this way are never stable. For each phase considered, the program starts with fully saturated magnetisation in every plane and iterates a mean-field equation until the magnetisations stop changing. It then calculates the mean-field free energy; the free energies of the phases are compared to establish the stability of the child phase and its lines of coexistence with its parents. Many of the phases found by the program are too narrow to be visible in the figure; others may be too narrow for the program, with finite precision, to find. Because mean-field theory cannot distinguish ⟨$\bar{2}$⟩ from ⟨2⟩ (the difference involving a correlated excitation of two spins), the phases ⟨2^k3⟩ are found to come in. Otherwise, there is good agreement with the low-temperature expansion presented in the text.

At $x = \frac{1}{3}$, (2) and (3) coexist, but no other phases are stable†. Contrast this with the *multiphase point* at $x = 1$, where infinitely many phases coexist. These are states for which the difference, $|n_{i+1} - n_i|$, between successive planes of spins is always either 1 or 2 with the proviso that a 'skip' of 2 cannot be followed immediately by another skip of 2. The antiferromagnetic coupling J_2 requires furthermore that the entire chain should maintain one helicity: the difference in spins between successive layers is always positive for the whole chain or else always negative. In addition to these states, the phase (5) also has the same energy at this ratio of the axial couplings.

To label these phases (except for (5)) in a way consistent with previous work on the anisotropic next-nearest-neighbour Ising (ANNNI) model (Fisher and Selke 1980, 1981, Fisher and Szpilka 1987a, 1987b, Szpilka and Fisher 1986, 1987, Yeomans 1988, Selke 1992) we say there is a *wall* between two successive planes when their spins differ by 2 instead of by 1. Two walls k spins apart are said to bound a k-band. A state is labelled by $\langle k_1 k_2 k_3 \ldots \rangle$ if it comprises a repeating sequence of bands of lengths

† We briefly discuss below the phase 45001233, which comes very close in energy to the phases (2) and (3) at $x = \frac{1}{3}$ and which actually becomes the stable phase at a sufficiently high temperature.

$k_1, k_2, k_3, \ldots$. It may be helpful to list examples of phases degenerate at $x=1$ together with their labels. Walls are indicated by vertical lines:

$$\langle 2 \rangle \qquad \ldots 01|34|01|34\ldots \tag{6}$$

$$\langle 2^2 3 \rangle \qquad \ldots 01|34|012|45|12|450\ldots \tag{7}$$

$$\langle 34 \rangle \qquad \ldots 012|4501|345|1234\ldots. \tag{8}$$

At $J_2=J_1$ ($x=1$), the energy cost in terms of the nearest-neighbour axial bond J_1 of introducing a wall is exactly balanced by the energy benefit to the next-nearest-neighbour interaction J_2, provided there are not two successive walls. Thus all states describable in this language that do not contain a 1-band are degenerate at $x=1$. The phase (5), which cannot be described within this notational scheme, is also degenerate at $x=1$; we label it $\langle \bar{2} \rangle$.

Now the six-state clock chain $\langle \infty \rangle$ with no walls has energy per spin $-\frac{1}{2}zJ_0-\frac{1}{2}J_1-\frac{1}{2}J_2$, where $z>2$ is the number of nearest neighbours a spin has in its own plane. As our model is relevant to rare-earth metals, we shall mostly be interested in $z=6$ (Jensen and Mackintosh 1991). The energy cost of adding an isolated wall, e.g. of changing 01234... to 012|45..., is $J_1-J_2=J_1(1-x)$. So long as walls are always at least two layers apart (no 1-bands), they *are* isolated, at zero temperature, giving for the energy per spin of a state with a density of walls W per plane

$$E_0=-\tfrac{1}{2}zJ_0-\tfrac{1}{2}J_1(1+x)+J_1(1-x)W. \tag{9}$$

To confirm our earlier assertions about the ground states, note that for $x<1$, E_0 is minimized by setting the wall density to zero, yielding the $\langle \infty \rangle$ phase, while for $x>1$, walls are favoured up to the maximum permitted density, one wall every two layers, giving the $\langle 2 \rangle$ phase.

While E_0 depends solely on the parameter W, we shall need to know more about the structures to determine their free energies at non-zero temperatures. It is helpful to follow Fisher and Selke (1980, 1981) and introduce variables $l_{k_1k_2k_3\ldots}$, defined as the number of times per spin the band-sequence $k_1k_2k_3\ldots$ appears in a given state. For example, for $\langle 223 \rangle$ (equation (7)),

$$l_2=\tfrac{2}{7} \qquad l_3=\tfrac{1}{7} \qquad l_{23}=\tfrac{1}{7} \qquad l_{2^23}=\tfrac{1}{7}. \tag{10}$$

The total wall density W is simply the sum of all the single-band structural variables, $\Sigma_{k\geq 2} l_k$. In the $\langle 2 \rangle$ phase, $l_2=\frac{1}{2}$, while l_k for $k=3, 4, 5, \ldots$ is zero.

3. Low-temperature series: first order

Our aim is to understand which of the degenerate states persist at non-zero temperature around the multiphase point, $x=1$. To this end we perform a low-temperature expansion around all possible ground states following the method of Fisher and Selke (1980, 1981).

The low-temperature expansion follows as usual from a decomposition of the partition function (Domb 1960). Consider a ground state with energy E_0. Now consider the excitation caused by flipping some finite number of spins, which can be either connected by bonds or disconnected. Let the ith such excitation have an energy cost relative to the ground state of E_i, and for a fixed ground-state configuration let there be g_i ways of placing it on the lattice.

The linked cluster theorem (Domb 1960) establishes that one can write the free energy per spin in terms of the energies E_i and counts g_i as

$$f = E_0 - k_B T \sum_{i=1}^{\infty} \gamma_i \, e^{-\beta E_i} \tag{11}$$

where γ_i, is the *intensive* part of the count per spin and β is the inverse temperature, $1/k_B T$. For a connected excitation, g_i is proportional to the number of spins, N, so that $\gamma_i = g_i/N$. However, an unconnected excitation also has quadratic and higher powers of N; the difficult but physically necessary result of the linked-cluster theorem is that all of these cancel, leaving just the parts linear in N: $\gamma_i = \text{linear}(g_i)/N$.

The Boltzmann factors $\exp(-\beta E_i)$ are made up of the weights

$$w = e^{-(1/2)\beta J_0} \qquad y = e^{-(1/2)\beta J_1} \qquad \text{and } y^{-x} = e^{(1/2)\beta J_2} \tag{12}$$

for changing an in-plane, axial nearest neighbour, and axial second-nearest neighbour bond, respectively from one between two equal spins to one between spins differing by 1.

Table 1 lists the six different local environments for spins, their energies, and the Boltzmann weights (entropic contributions) associated with flipping each possible spin plus one clock direction and then minus one clock direction (these two have been added together in the last column). These entropic terms can stabilize phases at non-zero temperature. As a simple physical illustration, consider the phase $\langle 3 \rangle$. At $T=0$, it loses in energy to $\langle 2 \rangle$ (or $\langle \hat{2} \rangle$) to the right ($x>1$) of the multicritical point $x=1$ and to $\langle \infty \rangle$ to the left (equation (9)). However, none of these phases to which it loses can support the excitation labelled $\sigma^+|$ (the superscript indicating a flip in the positive sense, as defined by helicity, the bar a wall) in the left column of the table, as none has any sites σ, for which one requires a wall density W strictly less than $\frac{1}{2}$ but still greater than zero. Since phase $\langle 3 \rangle$ has the highest density of sites σ of any possible phase, it should spread out in both directions from the multicritical point, as its superior entropy dominates the fixed energy difference between it and its competitors. The excitation $\sigma^+|$ is rather simple; when we consider increasingly complicated excitations, generally involving spin flips on linked sites over some distance, more phases

Table 1. Limiting ourselves to the phases of interest near $J_2 = J_1$, we list the six possible local neighbourhoods for a spin, differing in whether their first- and second-neighbour bonds cross walls. We list the label (adopted from Fisher and Selke, 1981), an example, the density of such spins in a chain, the energy of the spin, and the sum of Boltzmann weights for flipping the spin plus and minus one clock direction. The densities are given in terms of the wall density W and the two structural variables l_2 (density of 2-bands) and l_3 (density of 3-bands); note that the third column sums to 1.

Label	Example	Density	E_0 per spin	Entropy
0	$01\hat{2}34$	$1-(4W-l_3-2l_2)$	$-\frac{1}{2}zJ_0-\frac{1}{2}J_1-\frac{1}{2}J_2$	$2y^{1+x}w^z$
π	$01\hat{2}3\|5$	$2(W-l_2-l_3)$	$-\frac{1}{2}zJ_0-\frac{1}{2}J_1-\frac{1}{4}J_2$	$(y+y^{1+3x})w^z$
ρ	$5\|1\hat{2}3\|5$	l_3	$-\frac{1}{2}zJ_0-\frac{1}{2}J_1-J_2$	$2y^{1+2x}w^z$
σ	$01\hat{2}\|45$	$2(W-l_2)$	$-\frac{1}{2}zJ_0-\frac{3}{4}J_2$	$(1+y^{3x})w^z$
τ	$5\|1\hat{2}\|45$	$2l_2$	$-\frac{1}{2}zJ_0-J_2$	$2y^{2x}w^z$
$\bar{\tau}$	$00\hat{3}30$	—[a]	$-\frac{1}{2}zJ_0-J_2$	$2y^{2x}w^z$

[a] This phase cannot be described in terms of the structural variables l_k.

will spring out, as in the ANNNI model (Fisher and Selke 1980, 1981, Fisher and Szpilka 1987a, 1987b).

We could proceed by fixing the ratio J_0/J_1 at some value and simply list all the possible excitations, in order of increasing energy cost, along with their entropies. While this is relatively straightforward for the first dozen or so excitations, we will take a more systematic approach and treat the series as an expansion in w^z, implicitly assuming that J_0 is sufficiently large compared to J_1; we defer to the end a brief discussion of the extent to which the argument can be modified to accommodate a J_0 that is not necessarily large. Only flips of a single clock direction ($n_{i\alpha} \to n_{i\alpha} \pm 1$) need be considered in low order, with correction terms of order w^{3z} for flips of two clock directions.

We consider now all such excitations of a single spin, that is all excitations coming in with a weight w^z times some power of y. Whereas the 'zeroth-order' result for the energy (f at $T=0$) in (9) depended solely on the wall density W, to first order we require the additional structural variables l_2 and l_3. Reading off the free energy per spin directly from table 1, we have

$$\begin{aligned} f = &-\tfrac{1}{2}zJ_0 - \tfrac{1}{2}J_1(1+x) \\ &+ J_1 W(1-x) - k_B T w^z[(1-4W+l_3+2l_2)2y^{1+x} + 2(W-l_2-l_3)(y+y^{1+3x}) \\ &+ 2l_3 y^{1+2x} + 2(W-l_2)(1+y^{3x}) + 4l_2 y^{2x}] + O(w^{2z-2}) \end{aligned} \tag{13}$$

where the correction term arises from flips of two connected in-plane neighbours.

The coexistence line of $\langle 2 \rangle$ and $\langle 3 \rangle$ is recovered by setting to zero the difference between their free energies, $f_{\langle 2 \rangle} \equiv f(W = l_2 = \frac{1}{2},\ l_3 = 0)$ and $f_{\langle 3 \rangle} \equiv f(W = \frac{1}{3},\ l_2 = 0,\ l_3 = \frac{1}{3})$:

$$x_{\langle 3 \rangle : \langle 2 \rangle} = 1 + \frac{4k_B T}{J_1} w^z (1 + y^{3x} + y^{1+2x} - 3y^{2x}) + O(w^{2z-2}). \tag{14}$$

Similarly,

$$x_{\langle 4 \rangle : \langle 3 \rangle} = 1 - \frac{2k_B T}{J_1} w^z (1 - 3y + 4y^{1+2x} + y^{3x} - 3y^{1+3x}) + O(w^{2z-2}) \tag{15}$$

and

$$x_{\langle \infty \rangle : \langle 4 \rangle} = 1 - \frac{2k_B T}{J_1} w^z (1 + y - 4y^{1+x} + y^{3x} + y^{1+3x}) + O(w^{2z-2}). \tag{16}$$

The free-energy difference between the $\langle \infty \rangle$ phase and any phase $\langle k \rangle$, $k \geq 4$, is linear in W: therefore all of these phases coexist on the boundary defined by equation (16), although they do not occupy any area in the phase diagram. All phases containing 3- and 4-bands are degenerate on the coexistence line (15), and all phases containing 2- and 3-bands on (14), to this order.

Reading from the last two rows of table 1, we see that the free energy of $\langle \bar{2} \rangle$ is identical to that of $\langle 2 \rangle$. Therefore, to this order, they remain degenerate at all temperatures. To break this degeneracy, and those on the phase boundaries (14)–(16), higher-order terms in the low-temperature expansion are needed.

4. Low-temperature series: higher orders

The $\langle \bar{2} \rangle$–$\langle 3 \rangle$ region

No flip of a single spin can distinguish the phases $\langle 2 \rangle$ and $\langle \bar{2} \rangle$: the excitation comes in

with the same energy and degeneracy in the two phases. Nor for the same reason can the next highest-cost excitation, the flipping of two neighbouring spins in the same plane in the same direction. One sees, furthermore, that the global spin rotation on the odd (or even) sublattice taking 00|33|00|33 into 01|34|01|34 leaves invariant the energy (and obviously the count) of any spin excitation residing solely on one or the other sublattice†.

However, as soon as we consider flipping two axially-connected spins in neighbouring planes, we find one phase favoured. In the $\langle\bar{2}\rangle$-phase chain 00|33|00, a spin flip ± 1 of any connected pair on successive planes between walls costs energy $zJ_0 - J_1 + 2J_2$. This is the lowest-energy excitation involving two connected spins in adjacent planes, and it has a degeneracy of 1 per spin. The chain 01|34|01 supports an excitation of the same energy, but with one half the degeneracy. Therefore $\langle\bar{2}\rangle$ always wins over $\langle 2\rangle$ at sufficiently low temperatures.

In table 2, we collect the densities and Boltzmann weights for all two-spin excitations. Noting that in the $\langle 2\rangle$ phase $l_2 = \frac{1}{2}$ and $l_3 = 0$, we see that the difference in free energies between it and the $\langle\bar{2}\rangle$ phase is

$$f_{\langle\bar{2}\rangle} - f_{\langle 2\rangle} = -\tfrac{1}{2} k_B T w^{2z} y^{4x} (y^{-2} - y^{-1} - y + y^2) + O(w^{3z}) \tag{17}$$

which in this order is always negative, as y is strictly less than unity.

Now it is possible to use the information given in table 2 to check if new phases appear between $\langle\bar{2}\rangle$ and $\langle 3\rangle$ at second order. Previous work (Fisher and Selke 1980, 1981) has suggested that the first phase to consider is $\langle 23\rangle$, and indeed this is the only phase made up of 2- and 3-bands that could be distinguished by two spin flips. For $\langle 23\rangle$, $l_2 = l_3 = \frac{1}{5}$. Hence, to leading order, the free-energy difference between the candidate phase and its parents, evaluated at the coexistence line between the parents, is‡

$$f_{\langle 23\rangle} - \tfrac{2}{5} f_{\langle\bar{2}\rangle} - \tfrac{3}{5} f_{\langle 3\rangle} = -\tfrac{1}{5} k_B T w^{2z} (3 - 3y - 14y^2 + 21y^3 + 5y^4 - 22y^5 + 12y^6 - 2y^7) + O(w^{3z}) \tag{18}$$

This is negative at low temperature, and we can conclude that $\langle 23\rangle$ appears as a stable phase of width $O(w^{2z})$ between $\langle 3\rangle$ and $\langle\bar{2}\rangle$. (In this order (18) turns slightly positive for temperature over about $1.358 J_1/k_B$, but at this temperature the low-temperature series cannot be trusted. We expect the phase to remain stable at higher temperatures; see figure 1.)

It is not hard to argue that no other phases can appear between $\langle\bar{2}\rangle$ and $\langle 23\rangle$.

† This is because the J_2 (second-axial-neighbour) bonds are invariant under the transformation, while the sum of the two J_1 bonds cancels, since the two axial neighbours of any spin are left π radians out of phase, and $\cos(x) + \cos(\pi - x) = 0$.

‡ The construction of equation (18) obviates the need to consider the left and right boundaries separately. We see from equation (13) that for two phases c and d, $f_c - f_d$ is to first order linear in $W_c - W_d$ (using $W = l_2 + l_3 = (1/3)(l_2 + 1)$); from the values of W for the three phases, it follows that the left-hand side of (18), evaluated at *any* x, vanishes in first order. In particular, all first-order terms vanish when we look for the new phase along the (previous-order) coexistence line of the two parent phases by substituting $x = x_{\langle 3\rangle;\langle 2\rangle}$ (equation (14)). Now if instead of $x = x_{\langle 3\rangle;\langle 2\rangle}$ we substitute $x = 1$ (which is easier), we make an error in the second-order terms only (the zeroth and first having vanished) of order $w^z w^{2z} = w^{3z}$, which we may neglect. This construction generalizes to higher orders; see Fisher and Selke (1981).

Table 2. We list all two-spin excitations that are possible on the $\langle 3\rangle:\langle\bar{2}\rangle$ boundary: we thus have $l_k=0$ for $k\geqslant 4$. Note also that at least one of l_{22} and l_{33} vanishes. The local environment symbols ρ, σ, τ, and $\bar{\tau}$ are as in table 1. We denote by $\circ;\circ$ two entirely independent excitations; for these, the count is not the full count but only that part linear in N (see text). The other symbols convey information about the environment of the two spins flipped. The symbol $\circ\circ$ means two neighbouring spins on a single plane, $\circ,\circ$ axial nearest neighbours not separated by a wall, $\circ/\circ$ axial nearest neighbours separated by a wall, and $\circ\cdot\circ$ next-nearest axial neighbours. The last five rows of the table concern the phase $\langle\bar{2}\rangle$.

Configuration	Count per spin	Boltzmann factor
$\rho;\rho$	$-\frac{1}{6}(z+1)(1-2l_2)$	$4w^{2z}y^{2+4x}$
$\sigma;\sigma$	$-(1-2l_2)(1+z/3)+l_{23}$	$w^{2z}(1+y^{3x})^2$
$\tau;\tau$	$-l_2(5+z)+3l_{23}$	$4w^{2z}y^{4x}$
$\rho;\sigma$	$-\frac{1}{3}(4-8l_2-6l_{23})$	$2w^{2z}y^{1+2x}(1+y^{3x})$
$\rho;\tau$	$-2l_{23}$	$4w^{2z}y^{1+4x}$
$\sigma;\tau$	$-4l_{23}$	$2w^{2z}(1+y^{3x})y^{2x}$
$\rho\rho$	$\frac{1}{6}z(1-2l_2)$	$2(w^{2z-2}+w^{2z+1})y^{2+4x}$
$\sigma\sigma$	$\frac{1}{3}z(1-2l_2)$	$w^{2z-2}(1+y^{6x})+2w^{2z+1}y^{3x}$
$\tau\tau$	zl_2	$2(w^{2z-2}+w^{2z+1})y^{4x}$
ρ,σ	$\frac{2}{3}(1-2l_2)$	$w^{2z}(2y^{2x}+y^{5x}+y^{3+5x})$
τ,τ	l_2	$w^{2z}(3y^{-1+4x}+y^{2+4x})$
σ/σ	$\frac{1}{3}-\frac{2}{3}l_2-l_{23}$	$w^{2z}(y+2y^{1+3x}+y^{-2+6x})$
σ/τ	$2l_{23}$	$w^{2z}(2y^{1+2x}+y^{-2+5x}+y^{1+5x})$
τ/τ	l_2-l_{23}	$w^{2z}(y^{-2+4x}+3y^{1+4x})$
$\sigma\cdot\sigma$	$\frac{1}{3}(1-2l_2)$	$w^{2z}(3y^{2x}+y^{5x})$
$\rho\cdot\sigma$	$2(\frac{1}{3}-\frac{2}{3}l_2-l_{23})$	$w^{2z}(y+2y^{1+3x}+y^{1+6x})$
$\rho\cdot\tau$	$2l_{23}$	$w^{2z}(2y^{1+2x}+2y^{1+5x})$
$\sigma\cdot\tau$	$2l_{23}$	$w^{2z}(1+2y^{3x}+y^{6x})$
$\tau\cdot\tau$	$2(l_2-l_{23})$	$w^{2z}(2y^{2x}+2y^{5x})$
$\bar{\tau};\bar{\tau}$	$-\frac{1}{2}(5+z)$	$4w^{2z}y^{4x}$
$\bar{\tau}\bar{\tau}$	$\frac{z}{2}$	$2(w^{2z-2}+w^{2z+1})y^{4x}$
$\bar{\tau},\bar{\tau}$	$\frac{1}{2}$	$w^{2z}(2y^{-2+4x}+2y^{1+4x})$
$\bar{\tau}/\bar{\tau}$	$\frac{1}{2}$	$w^{2z}(2y^{-1+4x}+2y^{2+4x})$
$\bar{\tau}\cdot\bar{\tau}$	1	$w^{2z}(2y^{2x}+2y^{5x})$

Candidates are states made up of 2-bands and 23-sequences. Consider a state $\langle\nu\rangle$ with k_2 of the former and k_{23} of the latter. Then

$$f_{\langle\nu\rangle}-\frac{2k_2}{2k_2+5k_{23}}f_{\langle 2\rangle}-\frac{5k_{23}}{2k_2+5k_{23}}f_{\langle 23\rangle} \tag{19}$$

is $O(w^{3z})$. It follows from equation (17) that

$$f_{\langle\nu\rangle}-\frac{2k_2}{2k_2+5k_{23}}f_{\langle\bar{2}\rangle}-\frac{5k_{23}}{2k_2+5k_{23}}f_{\langle 23\rangle} \tag{20}$$

is $O(w^{2z})$ and positive. Hence the $\langle\bar{2}\rangle:\langle 23\rangle$ coexistence line marks a first-order transition rather than a multicritical line, and no other phases spring from it at zero temperature.

To put the same argument more physically, the excitation $\sigma^+\cdot\tau^+$ (table 2), which favours the $\langle 23\rangle$ phase over the two parents, has a lower energy cost than the $\bar{\tau},\bar{\tau}$ excitation responsible for $\langle\bar{2}\rangle$'s stability over $\langle 2\rangle$. This latter, however, costs less than

the three-spin excitation that would favour $\langle 223\rangle$ or those that would bring in more complicated mixed phases. Therefore these fail to attain stability†.

Consider now the boundary between $\langle 23\rangle$ and $\langle 3\rangle$ where, to second order in w^z, all phases containing only 3-bands and 23-sequences are degenerate. It is expected from previous analytic and numerical work (Fisher and Selke 1980, 1981, Fisher and Szpilka 1987a, 1987b, Duxbury and Selke (1983) and Selke and Duxbury (1984)) that the first phase to appear between $\langle 23\rangle$ and $\langle 3\rangle$ is $\langle 233\rangle = \langle 23^2\rangle$. Consider the free-energy difference per spin

$$a_{23^2} = f_{\langle 23^2\rangle} - \tfrac{5}{8} f_{\langle 23\rangle} - \tfrac{3}{8} f_{\langle 3\rangle}. \tag{21}$$

The leading terms in this quantity are third order (the free energies being degenerate in lower orders), arising from excitations of three axially-connected second-neighbour spins together with their associated disconnections. These are the lowest-order graphs that span all the bands of $\langle 23^2\rangle$. Therefore it is intuitively reasonable that they are the first graphs to distinguish $\langle 23^2\rangle$ and phases of shorter wavelength.

Because one-dimensional chains of spins provide the leading-order contribution to free-energy differences such as (21), their values can be calculated using a transfer-matrix approach first described by Yeomans and Fisher (1984). Details of its application to this problem are given in the appendix. One finds that the free-energy difference (21) is, to leading order in w

$$a_{23^2} = -4\frac{k_B T}{8} w^{3z} y(1 - y - 3y^2 + 3y^3 + 4y^4 - 6y^5 + y^6 + 3y^7 - 3y^8 + y^9) \tag{22}$$

which is negative. Hence $\langle 23^2\rangle$ is stable over a region $O(w^{3z})$ between $\langle 23\rangle$ and $\langle 3\rangle$.

The argument continues inductively on each phase boundary. It will be helpful to define $n(\nu)$ as the number of spins in the sequence ν. Consider two neighbouring phases $\langle \nu_1\rangle$ and $\langle \nu_2\rangle$ such that on the boundary between them all states made up from ν_1-sequences and ν_2-sequences are degenerate at a given order of the low-temperature series expansion. Our aim is to investigate which phases can appear between $\langle \nu_1\rangle$ and $\langle \nu_2\rangle$ at higher orders of the expansion. Let ν comprise p_1 ν_1-sequences and p_2 ν_2-sequences (in any order). Then consider

$$a_\nu = f_{\langle \nu\rangle} - \frac{p_1 n(\nu_1)}{p_1 n(\nu_1) + p_2 n(\nu_2)} f_{\langle \nu_1\rangle} - \frac{p_2 n(\nu_2)}{p_1 n(\nu_1) + p_2 n(\nu_2)} f_{\langle \nu_2\rangle}. \tag{23}$$

It is not difficult to show by construction, and it is intuitively reasonable, that the diagrams in the low-temperature series that do not drop out when the free energy difference is taken must comprise connected spin flips spanning at least $n(\nu) - 3$ axial planes (together with their disconnections). Of these, those contributing at lowest order are axial chains of spins. For $n(\nu)$ even, the flipped spins must all be second neighbours, and the leading term in (23) is $Ow^{(m(\nu)-2)/2}$)‡. For $n(\nu)$ odd, chains of

† The obvious question arises, 'what happened to the multiphase line on which, in a given order n, all sufficiently long ($m \geq n$) phases $\langle 2^m 3\rangle$ were degenerate?' In fact it is still there, but for the reason just given it lies to the right of the $\langle 23\rangle$:$\langle \bar{2}\rangle$ line, well inside the $\langle \bar{2}\rangle$ phase. We discuss later how sufficiently low J_0 or high temperature can stabilize these phases.

‡ Flipping only second-neighbour spins gives the shortest connected excitation spanning the given length. Of course, if we found that the free-energy difference a vanished in some case, we would have to consider chains of the same length but with more spins flipped. We prove in the appendix that this does not occur.

length $n(\nu)-3$ with one first-neighbour pair of flipped spins and those of length $n(\nu)-2$ with only second-neighbour flips both contribute at leading order, $O(w^{(n(\nu)-1)/2})$. A more detailed description of which axial chains are important, together with a description of how to calculate the corresponding Boltzmann factors using a transfer matrix method, is given in appendix 1. Because it corresponds to the smallest $n(\nu)$, the first phase that could appear between $\langle\nu_1\rangle$ and $\langle\nu_2\rangle$ is $\langle\nu_1\nu_2\rangle$. If $a_{\langle\nu_1\nu_2\rangle}$ is negative, it will be stabilised within a region $O(w^{(n(\nu_1\nu_2)-2)/2})$ of the $\langle\nu_1\rangle:\langle\nu_2\rangle$ boundary. Higher-order phases comprising ν_1- and $\nu_1\nu_2$-sequences and ν_2- and $\nu_1\nu_2$-sequences will remain degenerate on the $\langle\nu_1\rangle:\langle\nu_1\nu_2\rangle$ and $\langle\nu_2\rangle:\langle\nu_1\nu_2\rangle$ boundaries respectively, and the argument must recommence. If $a_{\nu_1\nu_2}$ is positive, however, $\langle\nu_1\nu_2\rangle$ has a higher free energy than either $\langle\nu_1\rangle$ or $\langle\nu_2\rangle$ and cannot appear as a stable phase. The $\langle\nu_1\rangle:\langle\nu_2\rangle$ boundary then remains stable to all orders of the low-temperature series expansion.

In the appendix, we derive a general form for the leading order in w of all the free-energy differences a_{23^k}, $a_{23^k1^23^k}$, $a_{23^k1^23^k1^23^k}$, etc. Specializing to the leading order in y as well as w, we show that these, and indeed the free-energy differences relevant to the *entire hierarchy* of phases between $\langle\infty\rangle$ and $\langle 23\rangle$, are always negative at sufficiently low temperature. Therefore *every phase is stable* at low enough temperature in some finite region of the J_2/J_1–T phase space.

Related issues

The expansion made here tells us accurately what happens at sufficiently low temperatures but gives only limited information about possible higher-temperature phases. For comparison, we show in figure 1 a phase diagram derived from mean-field theory, which we will discuss in more detail elsewhere. The main difference between the mean-field treatment and that presented here is the failure of mean-field theory to distinguish between the $\langle 2\rangle$ and $\langle\bar{2}\rangle$ phases. Also, a numerical solution of the theory precludes finding the arbitrarily narrow mixed phases discussed above.

We have assumed $zJ_0 \geq J_1$. Cooper (1962, 1968) has shown, however, that in some rare earths J_0 is of the order of 1/50 J_1. In fact, many of the qualitative results carry through to this regime, in which the expansion parameter is y instead of w. The excitations responsible for stabilising some of the low-order phases (see (14)–(16) and (18)) do not involve any broken J_1 or J_2 bonds (powers of y): therefore the first few terms of the expansion (11) are just successive powers of w. It is interesting to note that the phases $\langle 2^n3\rangle$ appear in this regime. There is one class of chains that can have arbitrary length before any J_1 or J_2 bonds are broken; this is $\sigma\cdot\tau\cdot\tau\cdot\ldots$. Such chains stabilize the phases $\langle 2^n3\rangle$ at an (infinitely) lower energy, for infinitesimal J_0, than the excitation responsible for $\langle\bar{2}\rangle$'s stability over $\langle 2\rangle$. Thus, if we are willing to contemplate a sufficiently small J_0, a finite number of these phases do come in at arbitrarily low temperature. Comparing the energies of the excitations, we find that for $zJ_0 \leqslant 2J_1/(n-1)$, the phase $\langle 2^n3\rangle$ becomes stable. These and mixed phases may also appear for larger J_0 at higher temperature; however, it is not clear that the low-temperature expansion continues to be valid here.

Although we have concentrated on the multiphase point $x=1$, it is worth noting that the ferromagnetic-helical boundary at $x=\frac{1}{3}$ (at zero temperature) comes very close to being a multicritical point; the phase 00 12 33 45 has an energy per spin only $J_1/24$ higher than the ferromagnetic and helical phases at that point. Furthermore, it

supports an excitation of lower energy than any found in either of the latter and so might be expected to acquire stability on entropic grounds at a sufficiently high temperature. If we set $z=6$, the new phase comes in at temperatures $k_B T$ around $2J_1$ for $J_0/J_1=1$ and at $0.13J_1$ for $J_0/J_1=1/50$. Higher-energy excitations favour this phase over similar phases, such as 00 123 44 501 . . . , so there is no multicritical point nor any infinite branching of phases.

Sasaki (1992) has interpolated between the six-state clock model and the XY model by adding to the latter a variable six-fold anisotropy. Expanding about the point with infinite anisotropy, and adding an external field, he finds a very rich phase diagram, including possible 'upsilon points' (Bassler *et al* 1991), even though his attention is restricted to zero temperature.

The model can be modified by alternating layers of some thicknesses of magnetic metals and non-magnetic conductors, through which the magnetic layers interact in a RKKY-like manner (Majkrzak *et al* 1991 and references therein, Deaven and Rokhsar 1991, Jones and Hanna 1993, Chen and Ko 1993). This interaction can be modelled with effective axial bond strengths J_1' and J_2'; it is then interesting to look for qualitatively new phases.

Acknowledgements

JMY was supported by a SERC Advanced Fellowship. FS was supported by a grant from the European Community through the SCIENCE programme. DAR was supported in part by the North Atlantic Treaty Organisation under a grant awarded in 1991 and by the SERC through grant GR/H73028.

Appendix 1. Transfer matrices

Our aim is to calculate free-energy differences such as (22). The leading-order contributions come from certain axial chains of flipped spins the associated Boltzmann factors of which can be most easily calculated using a transfer-matrix formalism. The basic idea is to calculate the entropy of a finite-spin excitation, of length about equal to the periodicity of the phase in question, as a finite product of matrices, each representing two spin flips. The matrix product sums over intermediate spin states, and vectors cap the product at each end. We refer the reader to Yeomans and Fisher (1984) and to Fisher and Szpilka (1987a) (especially sections III.A and III.B) for a more detailed account of the principles whose application we describe here.

Consider a spin sequence ν of length $n(\nu)$. To establish its stability (entropic advantage) over some parent phases will require a spin-excitation chain spanning ν's length. For an even-length sequence, the shortest such chain, and hence lowest-order in w, flips a spin in every second plane for a total of $\frac{1}{2}(n(\nu)-2)$ flipped spins. 2×2 transfer matrices can then be used to calculate the Boltzmann factors. If $n(\nu)$ is odd, however, chains of length $\frac{1}{2}(n(\nu)-1)$ are needed, and somewhere in the chain a single pair of flipped spins can lie in nearest-neighbour planes. 4×4 matrices then prove the most convenient.

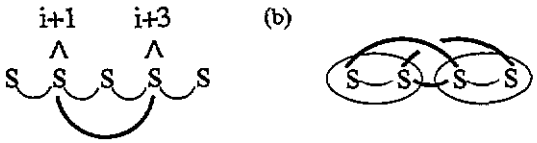

Figure 2. (a) A 2×2 matrix looks at spin flips in planes $i+1$ and $i+3$. The Boltzmann weight for the second-axial-neighbour bond between them, shown as a dark line, is counted at full strength, as only one matrix includes this bond. The first-axial-neighbour bonds, shown as lighter lines, are each counted by two matrices (this matrix and the one to the left or to the right). These therefore count at half strength, or the square root of the Boltzmann weight. (b) A 4×4 matrix flips one spin in each of the circled pairs. The two second-axial-neighbour bonds are counted at full strength, as is the first-axial-neighbour bond between the neighbouring planes of the two pairs. The first-axial-neighbour bond within each pair, however, counts at half strength.

A.1. n(v) even

We first construct the transfer matrix that looks at the effects of flipping two spins in next-nearest-neighbour planes $i+1$ and $i+3$ (figure 2(a)). The next matrix to the right will flip a spin in plane $i+3$ and another in plane $i+5$, while the matrix on the left of the first matrix will consider flips in planes $i-1$ and $i+1$. The Boltzmann weights of the four axial-nearest-neighbour bonds to the left and to the right of the two flipped spins come in at only half strength, as each will be counted by two matrices. The second-neighbour bond between the two flipped spins of a matrix, however, is counted only in that matrix and so has full strength. Each matrix additionally will count the z broken in-plane bonds in each of layers $i+1$ and $i+3$, again at half strength.

Since we have to consider disconnected as well as connected diagrams, the spins in layers $i+1$ and $i+3$ need not lie on an axial line. From the connected value, we therefore subtract (the sign a consequence of the linked-cluster theorem) the Boltzmann weight for the $i+1$ spin connecting to an unflipped $i+3$ spin and vice-versa. As we are interested in the matrices evaluated at $x=1$ (see main text), and for simplicity, we show the results with this substitution. The first matrix is

(i) *a wall just to the left of layer* $i+3$ ($s\hat{s}s|\hat{s}s$)

$$\mathscr{A}=w^z y^{1/2}\begin{pmatrix} 1-y^2 & y^3-y^2 \\ y^3-y^2 & 1-y^2 \end{pmatrix}. \tag{A.1}$$

The first (row) index of the matrix gives the change ($+1$ or -1) in the value, n_{i+1}, of the first spin, while the second (column) index gives that of the second spin, at $i+3$. The matrices for other environments follow similarly. Reading a chain from right to left looks the same as reading it from left to right, except that helicity (0543 . . . against 0123 . . .) is reversed. We therefore denote by a dagger (†) the duality operation of reversing plus and minus flips and also transposing rows (left index) and columns

(right index)†. The matrix corresponding to a wall just to the right of layer $i+1$ ($s\hat{s}|s\hat{s}s$) is then $\mathscr{A}^\dagger = \mathscr{A}$. The other matrices are:

(ii) *a wall just to the right of layer* $i+3$ ($s\hat{s}s\hat{s}|s$)

$$\mathscr{C} = w^z y^{1/2} \begin{pmatrix} 1-y & y^3-y^4 \\ 1-y^{-2} & 1-y \end{pmatrix} \tag{A.2}$$

(iii) *no walls affecting any of the bonds under consideration* ($s\hat{s}s\hat{s}s$)

$$\mathscr{D} = y^{1/2}\mathscr{C} \tag{A.3}$$

(iv) *walls immediately to the right of both flipped layers,* $i+1$ *and* $i+3$ ($s\hat{s}|s\hat{s}|s$)

$$\mathscr{E} = y^{-1/2}\mathscr{A} \tag{A.4}$$

(v) *walls immediately to the left of* $i+1$ *and to the right of* $i+3$ ($s|\hat{s}s\hat{s}|s$)

$$\mathscr{F} = y^{-1/2}\mathscr{C}. \tag{A.5}$$

Each of these matrices is self-dual.

The following column vectors account for the contribution associated with the last (rightmost) flipped spin in a chain, contracting the last index of the matrix product. All the other broken bonds having been included already in this matrix product, these vectors describe only the nearest-axial-neighbour bonds to the left and right of that last spin (counted at half strength) and the second-neighbour axial bond heading to the right:

(i) *a wall lies two layers to the right of the flipped spin* ($s\hat{s}s|s$)

$$\boldsymbol{\beta} = w^{(1/2)z} y^{1/2} \begin{pmatrix} y \\ y \end{pmatrix} \tag{A.6}$$

(ii) *a wall lies immediately to the left of the flipped spin* ($s|\hat{s}ss$)

$$\boldsymbol{\gamma} = w^{(1/2)z} \begin{pmatrix} y^2 \\ y^{-1} \end{pmatrix} \tag{A.7}$$

(iii) *no walls lie within bonding range of the flipped spin* ($s\hat{s}ss$)

$$\boldsymbol{\delta} = y^{1/2}\boldsymbol{\gamma} \tag{A.8}$$

(iv) *walls lie immediately to the left and two layers to the right* ($s|\hat{s}s|s$)

$$\boldsymbol{\varepsilon} = y^{-1/2}\boldsymbol{\beta} \tag{A.9}$$

the upper element of each vector is obtained from $\Delta n = +1$, the lower from -1. As these spins lie on the end of a chain, there is no separate disconnection term.

Row vectors are needed to account for the contribution associated with the first (left-most) flipped spin of the chain; they are minus the dagger-conjugates of the column vectors, $-\boldsymbol{\gamma}^\dagger = w^{(1/2)z}(y^{-1}\ y^2)$, for instance, representing a wall immediately to the right of the leftmost flipped spin in the chain.

To apply this matrix method to the free-energy difference

$$a_{23^2} = f_{23^2} - \tfrac{5}{8} f_{23} - \tfrac{3}{8} f_3 \tag{21}$$

† This has the effect of reversing upper-left and lower-right elements. We define $X\dagger = (QXQ)^T$, where Q is the matrix with -1 along the antidiagonal. The sign has no effect on matrices but will be convenient when we act on vectors.

we consider the two diagrams involving the smallest number of flipped spins that distinguish $\langle 233\rangle$ from its parents $\langle 23\rangle$ and $\langle 3\rangle$,

$$s|s\hat{s}|s\hat{s}s|\hat{s}ss| \qquad -\boldsymbol{\varepsilon}^{\dagger}\mathcal{A}^{\dagger}\mathcal{A}\boldsymbol{\gamma} \tag{A.10}$$

and

$$|ss\hat{s}|s\hat{s}s|\hat{s}s|s \qquad -\boldsymbol{\gamma}^{\dagger}\mathcal{A}^{\dagger}\mathcal{A}\boldsymbol{\varepsilon} \tag{A.11}$$

where the spins are represented with letters s and the walls with vertical bars. We then subtract the diagrams

$$s|s\hat{s}|s\hat{s}s|\hat{s}s|s \qquad -\boldsymbol{\varepsilon}^{\dagger}\mathcal{A}^{\dagger}\mathcal{A}\boldsymbol{\varepsilon} \tag{A.12}$$

and

$$|ss\hat{s}|s\hat{s}s|\hat{s}ss| \qquad -\boldsymbol{\gamma}^{\dagger}\mathcal{A}^{\dagger}\mathcal{A}\boldsymbol{\gamma} \tag{A.13}$$

which occur in the parent phases but not in $\langle 23^2\rangle$, to give

$$a_{23^2}=-\frac{k_{\mathrm{B}}T}{8}(\boldsymbol{\gamma}-\boldsymbol{\varepsilon})^{\dagger}\mathcal{A}^2(\boldsymbol{\gamma}-\boldsymbol{\varepsilon}). \tag{A.14}$$

Note that the fractions multiplying f_{23} and f_3 in (22) give the densitities of these phases relative to f_{233}, causing all terms of lower-than-leading order to cancel. This generalizes for all even k to

$$a_{23^k}=-\frac{k_{\mathrm{B}}T}{2+3k}(\boldsymbol{\gamma}-\boldsymbol{\varepsilon})^{\dagger}\mathcal{A}(\mathcal{A}\mathcal{F}\mathcal{A})^{(k-2)/2}\mathcal{A}(\boldsymbol{\gamma}-\boldsymbol{\varepsilon}) \qquad k\geqslant 2 \text{ even}. \tag{A.15}$$

Diagonalizing the matrix, we get to leading order in y

$$a_{23^k}=-\frac{k_{\mathrm{B}}T}{2+3k}w^{(3k/2)z}y^{k/2}\left(\left[\frac{1}{2}-\frac{1}{\sqrt{3}}\right][2-\sqrt{3}]^{k/2}\right.$$
$$\left.+\left[\frac{1}{2}+\frac{1}{\sqrt{3}}\right][2+\sqrt{3}]^{k/2}+\mathrm{O}(y)\right) \qquad k\geqslant 2 \text{ even} \tag{A.16}$$

which is negative, establishing the stability of the $\langle 23^k\rangle$ phase over its parents at sufficiently low temperatures.

A.2. $n(v)$ odd

Consider now the case of an odd periodicity. While most of the time only every second spin will be flipped, in each chain there can be one pair of adjacent planes with flipped spins. To allow for this to occur anywhere (but only once) in the chain, we use 4×4 matrices; each represents four consecutive spins and counts half the weight of each of the first-axial-neighbour bonds between the first and second and between the third and fourth and the full weight of the two second-neighbour bonds between the first and third and between the second and fourth spins (figure 2(b)). It also counts zJ_0 to cover half the in-plane bonds of each flipped spin.

To avoid consideration of higher-order excitations than necessary, we will flip only one of the first and second spins and only one of the third and fourth. So long as we are careful with our choices of initial sites, this will entail no loss of generality. As with

the 2×2 matrices above, we evaluate the 4×4 matrices at $x=1$. Labelling the matrices by the quadruplets of spin differences for the four spins,

$$\begin{pmatrix} +0+0 & +0-0 & +00+ & +00- \\ -0+0 & -0-0 & -00+ & -00- \\ 0++0 & 0+-0 & 0+0+ & 0+0- \\ 0-+0 & 0--0 & 0-0+ & 0-0- \end{pmatrix} \tag{A.17}$$

where '+' and '−' indicate a difference ±1 and '0' no flip at all, we get:

(i) *a wall lying between the second and third layers* $(\hat{s}\hat{s}|\hat{s}\hat{s})$

$$\mathbf{A}=w^z\begin{pmatrix} 1-y^2 & -y^{1/2}+y^{3/2} & 0 & 0 \\ -y^{7/2}+y^{9/2} & 1-y^2 & 0 & 0 \\ -y^{3/2}+y^{5/2} & -1+y & 1-y^2 & -y^{1/2}+y^{3/2} \\ y-y^3 & -y^{3/2}+y^{5/2} & -y^{7/2}+y^{9/2} & 1-y^2 \end{pmatrix}. \tag{A.18}$$

The zero entries in the top right-hand corner come from third-neighbour (i.e. entirely disconnected) flips; physically, these diagrams were already considered in lower order and so cancel when we calculate a. The dual of a 4×4 matrix, written in terms of its 2×2 sub-blocks, is

$$\begin{pmatrix} X & 0 \\ Y & Z \end{pmatrix}^\dagger=\begin{pmatrix} Z\dagger & 0 \\ Y\dagger & X\dagger \end{pmatrix} \tag{A.19}$$

from which we see that **A** is self-conjugate, as indeed it must be from its geometry.

We shall also need the matrices:

(ii) *a wall lying between the first and second layers* $(\hat{s}|\hat{s}\hat{s}\hat{s})$

$$\mathbf{B}=w^z\begin{pmatrix} y^{1/2}-y^{5/2} & -y+y^2 & 0 & 0 \\ -y^4+y^5 & y^{1/2}-y^{5/2} & 0 & 0 \\ y^3-y^4 & -y^{5/2}+y^{9/2} & y^{1/2}-y^{3/2} & y^2-y^3 \\ y^{3/2}-y^{5/2} & 1-y & -1+y^2 & y^{1/2}-y^{3/2} \end{pmatrix} \tag{A.20}$$

(iii) *no walls inside the span of four layers* $(\hat{s}\hat{s}\hat{s}\hat{s})$

$$\mathbf{D}=w^z\begin{pmatrix} y-y^2 & y^{5/2}-y^{7/2} & 0 & 0 \\ -y^{1/2}+y^{5/2} & y-y^2 & 0 & 0 \\ y^{3/2}-y^{5/2} & -y^4+y^6 & y-y^2 & y^{5/2}-y^{7/2} \\ 1-y & y^{3/2}-y^{5/2} & -y^{1/2}+y^{5/2} & y-y^2 \end{pmatrix} \tag{A.21}$$

(iv) *walls between the first and second and between the third and fourth layers* $(\hat{s}|\hat{s}\hat{s}|\hat{s})$

$$\mathbf{E}=w^z\begin{pmatrix} 1-y^2 & -y^{1/2}+y^{3/2} & 0 & 0 \\ -y^{7/2}+y^{9/2} & 1-y^2 & 0 & 0 \\ y^{3/2}-y^{5/2} & -y+y^3 & 1-y^2 & -y^{1/2}+y^{3/2} \\ y^3-y^4 & y^{3/2}-y^{5/2} & -y^{7/2}+y^{9/2} & 1-y^2 \end{pmatrix}. \tag{A.22}$$

All the matrices except **B** are self-conjugate.

To account for the initial (leftmost) pair of spins, with both of their second-

neighbour bonds to the left (at full strength), the first-neighbour bond between the two of them (at half strength), and the first-neighbour bond to the left of the pair (at full strength), as well as the in-plane bonds (at half strength), we require row vectors:

(i) *a wall just to the left of the first flipped pair* $(ss|\hat{s}\hat{s})$

$$-\boldsymbol{a}^{\dagger}=w^{z/2}(y^{3/2}\ 1\ y^{2}\ y^{1/2}) \tag{A.23}$$

(ii) *a wall two positions to the left of the first flipped spin* $(s|s\hat{s}\hat{s})$

$$-\boldsymbol{b}^{\dagger}=w^{z/2}(y^{5/2}\ y\ 1\ y^{3/2}) \tag{A.24}$$

(iii) *no wall in range* $(ss\hat{s}\hat{s})$

$$-\boldsymbol{d}^{\dagger}=w^{z/2}(y^{1/2}\ y^{2}\ 1\ y^{3/2}). \tag{A.25}$$

To account for the right-most flipped spin pair we use the column-vector conjugates of these row vectors. For example, the spin configuration $\hat{s}\hat{s}s|s$ corresponds to

$$\boldsymbol{b}=w^{z/2}\begin{pmatrix} y^{3/2} \\ 1 \\ y \\ y^{5/2} \end{pmatrix}. \tag{A.26}$$

The simplest application of the 4×4 matrices is to the free-energy difference

$$a_{23^3}=f_{23^3}-\tfrac{8}{11}f_{23^2}-\tfrac{3}{11}f_3 \tag{A.27}$$

in which the diagrams

$$s|\widehat{s\ s}|\widehat{s\ s}\ \widehat{s}|\widehat{s}\ \widehat{s\ s}|\widehat{s\ s}\ s| \qquad -\boldsymbol{a}^{\dagger}\mathbf{A}\mathbf{B}^{\dagger}\mathbf{B}\mathbf{A}\boldsymbol{b} \tag{A.28}$$

and

$$|s\ \widehat{s\ s}|\widehat{s\ s}\ \widehat{s}|\widehat{s}\ \widehat{s\ s}|\widehat{s\ s}|s \qquad -\boldsymbol{b}^{\dagger}\mathbf{A}\mathbf{B}^{\dagger}\mathbf{B}\mathbf{A}\boldsymbol{a} \tag{A.29}$$

contribute to f_{23^3}, whilst

$$|s\ \widehat{s\ s}|\widehat{s\ s}\ \widehat{s}|\widehat{s}\ \widehat{s\ s}|\widehat{s\ s}\ s| \qquad -\boldsymbol{b}^{\dagger}\mathbf{A}\mathbf{B}^{\dagger}\mathbf{B}\mathbf{A}\boldsymbol{b} \tag{A.30}$$

and

$$s|\widehat{s\ s}|\widehat{s\ s}\ \widehat{s}|\widehat{s}\ \widehat{s\ s}|\widehat{s\ s}|s \qquad -\boldsymbol{a}^{\dagger}\mathbf{A}\mathbf{B}^{\dagger}\mathbf{B}\mathbf{A}\boldsymbol{a} \tag{A.31}$$

come from f_3 and f_{23^2}. One spin in each pair $(\hat{s}\hat{s})$ must be flipped such that the flipped spins are always either first or second neighbours. This allows for the possibility of one nearest-neighbour pair in the chain. We thus arrive at

$$a_{23^3}=-\frac{k_{\mathrm{B}}T}{11}(\boldsymbol{b}-\boldsymbol{a})^{\dagger}\mathbf{A}\mathbf{B}^{\dagger}\mathbf{B}\mathbf{A}(\boldsymbol{b}-\boldsymbol{a}). \tag{A.32}$$

More generally

$$a_{23^k}=-\frac{k_{\mathrm{B}}T}{2+3k}(\boldsymbol{b}-\boldsymbol{a})^{\dagger}\mathbf{A}\mathbf{B}^{\dagger}(\mathbf{B}\mathbf{A}\mathbf{B}^{\dagger})^{(k-3)/2}\mathbf{B}\mathbf{A}(\boldsymbol{b}-\boldsymbol{a}) \qquad k\geqslant3 \text{ odd}. \tag{A.33}$$

Now the matrix $\mathbf{BAB}^\dagger$ cannot be diagonalized, but we can still write its powers in terms of its eigenvalues, giving to leading order in y

$$a_{23^k} = -\frac{k_B T}{2+3k} w^{(3k+1)/2} y^{(k-1)/2} \left(\left[\frac{27+16\sqrt{3}}{18} + \frac{k-1}{2} \frac{(17+10\sqrt{3})}{12} \right] (2+\sqrt{3})^{(k-1)/2} + \left[\frac{27-16\sqrt{3}}{18} + \frac{k-1}{2} \frac{(17-10\sqrt{3})}{12} \right] (2-\sqrt{3})^{(k-1)/2} \right) \tag{A.34}$$

which again is always negative.

More complicated phases can be treated in an analogous way. For a phase $\langle 2\mu 3 \rangle$ where μ comprises 2- and 3-bands, contributions to the free-energy difference $a_{2\mu 3}$ arise from the sequences that span $2\mu 3$, $3\mu 2$, and with a negative sign for the parent phases, $3\mu 3$ and $2\mu 2$. For example,

$$a_{23^{k-1}23^k} = -\frac{k_B T}{1+6k} (\boldsymbol{b}-\boldsymbol{a})^\dagger \mathbf{A} (\mathbf{B}^\dagger \mathbf{B} \mathbf{A})^{(k-2)/2} \mathbf{B}^\dagger \mathbf{E} \mathbf{B} (\mathbf{A}\mathbf{B}^\dagger \mathbf{B})^{(k-2)/2} \mathbf{A} (\boldsymbol{b}-\boldsymbol{a}) \qquad k \geqslant 2 \text{ even} \tag{A.35}$$

$$a_{23^{k-1}23^k} = -\frac{k_B T}{1+6k} (\boldsymbol{b}-\boldsymbol{a})^\dagger \mathbf{A} (\mathbf{B}^\dagger \mathbf{B} \mathbf{A})^{(k-1)/2} (\mathbf{A}\mathbf{B}^\dagger \mathbf{B})^{(k-1)/2} \mathbf{A} (\boldsymbol{b}-\boldsymbol{a}) \qquad k \geqslant 3 \text{ odd.} \tag{A.36}$$

The formalism must be generalized slightly to treat the phases $\langle k \rangle$, $k \geqslant 3$, which appear between $\langle \infty \rangle$ and $\langle 3 \rangle$. The stability of $\langle k \rangle$ is controlled by

$$a_k \equiv f_k - \frac{k-1}{k} f_{k-1} - \frac{1}{k} f_\infty = -\frac{k_B T}{k} \times \begin{cases} (\boldsymbol{\delta}-\boldsymbol{\beta})^\dagger \mathfrak{D}^{(k-4)/2} (\boldsymbol{\delta}-\boldsymbol{\beta}) & k \geqslant 4 \text{ even} \\ (\boldsymbol{b}-\boldsymbol{a})^\dagger \mathbf{D}^{(k-3)/2} (\boldsymbol{b}-\boldsymbol{a}) + (\boldsymbol{\delta}-\boldsymbol{\beta})^\dagger \mathfrak{D}^{(k-3)/2} (\boldsymbol{\delta}-\boldsymbol{\beta}) & k \geqslant 5 \text{ odd} \end{cases} \tag{A.37}$$

where in the odd case we have used the identity $\boldsymbol{b}^\dagger \mathbf{D} \boldsymbol{b} = \boldsymbol{d}^\dagger \mathbf{D} \boldsymbol{d} - 2\boldsymbol{\delta}^\dagger \mathfrak{D} \boldsymbol{\delta} + \boldsymbol{\beta}^\dagger \mathfrak{D} \boldsymbol{\delta} + \boldsymbol{\delta}^\dagger \mathfrak{D} \boldsymbol{\beta}^\dagger$.

Again expanding $\mathbf{D}$ and $\mathfrak{D}$ in terms of their eigenvalues, we find that, to leading orders in y,

$$(\boldsymbol{\delta}-\boldsymbol{\beta})^\dagger \mathfrak{D}^n (\boldsymbol{\delta}-\boldsymbol{\beta}) \sim (n+1) w^{(n+1)z} y^{n+1}$$

and

$$(\boldsymbol{b}^\dagger - \boldsymbol{a}^\dagger) \mathbf{D}^n (\boldsymbol{b}-\boldsymbol{a}) \sim (n+2) w^{(n+1)z} y^n.$$

This establishes that a_k is negative at sufficiently low temperatures for all $k \geqslant 4$.

We are now in a position to show that all phases anywhere in the hierarchy between $\langle \infty \rangle$ and $\langle 23 \rangle$ are stable. Consider first a phase of even period. A general free-energy difference consists of a negative constant ($-k_B T$ divided by the period) times one of two row vectors, $(\boldsymbol{\gamma}-\boldsymbol{\varepsilon})^\dagger$ or $(\boldsymbol{\delta}-\boldsymbol{\beta})^\dagger$, followed by a product of 2×2 matrices, followed by the conjugate vector. The individual matrices (A.1)–(A.5) are each positive scalar multiples of either $\mathscr{A}$ or $\mathscr{C}$, so we consider only these two. Now we

† Note that the second term (last line) in (A.37) then serves in part to cancel a particular spin configuration that is counted twice in the first. Alternatively, one can rewrite the first line of (A.37) as $a_k = ((k+1/k)a_{k+1} + [f_k - ((k-1)/k)f_{k-1}] - ((k+1)/k)[f_{k+1} - (k/(k+1))f_k]$, which effectively substitutes $\langle k+1 \rangle$ for $\langle \infty \rangle$ as the left parent of $\langle k \rangle$, adding a_{k+1} as a correction for the difference between $\langle k+1 \rangle$ and $\langle \infty \rangle$. This case, the only one in which 4×4 and 2×2 matrices need to be mixed, is more complicated than the others because one cannot form the $\langle k \rangle$ phase by appending $\langle \infty \rangle$ to a period of phase $\langle k-1 \rangle$.

can find a basis in which, for sufficiently small y, only positive elements appear in the matrix product, ensuring that the final result is positive. One easily confirms that the matrix

$$\mathcal{U}=\mathcal{U}^{-1}=\begin{pmatrix}-1 & 0\\ 0 & 1\end{pmatrix} \tag{A.38}$$

transforms the two vectors (and consequently their duals) as well as the matrix $\mathcal{A}$, but not $\mathcal{C}$, into a form in which all their elements are positive. However, by diagonalizing $\mathcal{C}$, we get a general expression for $\mathcal{U}\mathcal{A}\mathcal{C}^k\mathcal{U}$, and it is not difficult to show that all elements of this matrix are positive at low enough temperature. Now the matrix $\mathcal{C}$ always occurs either in the combination $\mathcal{A}\mathcal{C}^k$, which we have just shown is made positive by $\mathcal{U}$, or immediately following one of the two row vectors (or preceding their duals). However, $(\gamma-\varepsilon)^\dagger\mathcal{C}\mathcal{U}$ and $(\delta-\beta)^\dagger\mathcal{C}\mathcal{U}$ are also both positive, so we have established that a_ν is negative for all phases $\langle\nu\rangle$ of even period.

We use a different argument for the 4×4 matrices appropriate to phases of odd period. The only vector we need (having eliminated d, see above) is $v=b-a$. One easily confirms that $v^\dagger v$ is positive for small enough y. We note two sufficient conditions on a column vector $u=(u_1\ u_2\ u_3\ u_4)^{\mathrm{T}}$ for $v^\dagger u$ also to be positive for small y†:

$$u_2\sim-u_3\sim-y^{-1/2}u_1>0 \tag{A.39}$$

and

$$y^{-1/2}u_2\gtrsim u_4\gg-y^{-1/2}u_2. \tag{A.40}$$

Note that v satisfies both conditions. Now assume that u satisfies the conditions. Showing that $u'=\mathbf{M}u$ also satisfies them for $\mathbf{M}=\mathbf{A}$, $\mathbf{B}$, $\mathbf{B}^\dagger$, $\mathbf{D}$, and $\mathbf{E}$, we establish by induction that all products of our matrices set between $v^\dagger$ and v give a positive result. We show this explicitly for A, omitting the rest of the proof in the interest of space.

Bearing in mind the two conditions, we have

$$u'=\mathbf{A}u=\begin{pmatrix}u_1-y^{1/2}u_2\\ u_2\\ -u_2+u_3-y^{1/2}u_4\\ u_4-y^{3/2}u_2\end{pmatrix}+\text{higher-order terms.} \tag{A.41}$$

We verify that u_2' remains positive, that u_1' and u_3' remain negative, that $u_1'\sim y^{1/2}u_3'$, that u_2' and u_3' have the same order (note carefully the $\gtrsim$ and the $\gg$ in (A.40)), and that u_4' stays within its bounds. The other four matrices follow similarly.

Since both even-period and odd-period matrix products are positive, the corresponding free-energy differences a are negative, and all phases attain a region of stability. Numerical calculation of the matrix products confirms this conclusion. We remark that the phases $\langle 2^k3\rangle$ fail to achieve stability not because of the matrices but because their free energies need to be compared with that of $\langle\bar{2}\rangle$ rather than of $\langle 2\rangle$. We note also that in determining the sign of the matrix products, we required specific information about the matrix and vector elements; an arbitrary product $w^\dagger Xw$ (even for X self-dual) is not in general positive. Indeed, in the ANNNI model (Fisher and Selke 1980, Fisher and Szpilka 1987), not all matrix products are positive.

† By $r\gtrsim q$, we mean $\lim_{y\to0}q/r=0$ if q is positive or $q/r\to\pm\infty$ if it is negative, while by $r\sim q$ we mean that q/r is positive, finite, and non-infinitesimal in this limit. The notation $r\gtrsim q$ then indicates that either $r\gtrsim q$ or else $r\sim q$. Note that u_1 is required to be negative, even though $(v\dagger)_1$ is positive.

References

Bassler K E, Sasaki K and Griffiths R B 1991 *J. Stat. Phys.* **62** 45
Chen N-N and Ko D Y K 1993 *Preprint*
Cooper B R 1962 *Proc. Phys. Soc. (London)* **80** 1225
—— 1968 *Solid State Phys.* **21** 393
Deaven D M and Rokhsar D S 1991 *Phys. Rev.* B **44** 5977
Domb C 1960 *Adv. Phys.* **9** 149
Duxbury P M and Selke W 1983 *J. Phys. A: Math. Gen.* **16** L741
Fisher M E and Selke W 1980 *Phys. Rev. Lett.* **44** 1502
—— 1981 *Phil. Trans. R. Soc. (London)* **302** 1
Fisher M E and Szpilka A M 1987a *Phys. Rev.* B **36** 644
—— 1987b *Phys. Rev.* B **36** 5343
Jehan D A, McMorrow D F, Cowley R A, Ward R C, Wells M R and Hagmann N 1993 *Preprint*
Jensen J and Mackintosh A R 1991 *Rare Earth Magnetism* (Oxford: Oxford University Press)
Jones B A and Hanna C B 1993 *Preprint*
Majkrzak C F, Kwo J, Hong M, Yafet Y, Gibbs D, Chien C L and Bohr J 1991 *Adv. Phys.* **40** 99
Sasaki K 1992 *J. Stat. Phys.* **68** 1013
Selke W 1992 *Phase Transitions and Critical Phenomena* vol 15, ed C Domb and J L Lebowitz (New York: Academic)
Selke W and Duxbury P M 1984 *Z. Phys.* B **57**, 49
Szpilka A M and Fisher M E 1986 *Phys. Rev. Lett.* **57** 1044
—— 1987 *Phys. Rev.* B **36** 5363
Yeomans J M 1988 *Solid State Physics* vol 41, ed H Ehrenreich and D Turnbull (New York: Academic) p 151
Yeomans J M and Fisher M E 1984 *Physica* **127A** 1
Yoshimori, A. 1959 *J. Phys. Soc. Japan* **14** 807